

# An ASCA observation of the radio-loud narrow-line Seyfert 1 galaxy RGB J0044+193

J. Siebert<sup>1,2</sup>, K.M. Leighly<sup>3</sup>, S.A. Laurent-Muehleisen<sup>4</sup>, W. Brinkmann<sup>1</sup>, Th. Boller<sup>1</sup>, and M. Matsuoka<sup>2</sup>

<sup>1</sup> Max-Planck-Institut für Extraterrestrische Physik, Giessenbachstrasse, D-85740 Garching, Germany

<sup>2</sup> Institute of Physical and Chemical Research (RIKEN), 2-1 Hirosawa, Wako, Saitama 351-01, Japan

<sup>3</sup> Columbia Astrophysics Laboratory, Columbia University, New York, NY 10027, USA

<sup>4</sup> IGPP/LLNL, 7000 East Av., Livermore, CA 94550, USA

Received 3 November 1998 / Accepted 24 February 1999

**Abstract.** Narrow-line Seyfert 1 galaxies are generally found to be radio-quiet and there was only one radio-loud object known so far (PKS 0558-504). Here we present the results of a 50 ksec ASCA observation of the recently discovered second radio-loud NLS1 galaxy RGB J0044+193. The X-ray data are complemented by radio observations and a new optical spectrum for this source.

We find evidence for variable radio emission and an inverted radio spectrum of RGB J0044+193. The optical continuum turned out to be extremely blue. This may either indicate additional line emission, for example from Fe I, or scattering of a blue intrinsic continuum. The X-ray spectrum shows a clear break around 1.8 keV. Above this energy the spectrum is characterized by a power law with a photon index of  $\Gamma \approx 2.1$ . For energies below 2 keV the spectrum is much softer and it can either be modeled with a steeper power law ( $\Gamma \approx 2.7$ ) or a blackbody component with a temperature around 0.2 keV. The X-ray count rate of the source decreased by a factor of two within one day and there is evidence for low amplitude variability on much shorter time scales. Given its average 2–10 keV X-ray luminosity of  $(1.35 \pm 0.05) \times 10^{44} \text{ erg s}^{-1}$ , RGB J0044+193 is significantly more variable than a typical broad line Seyfert 1 galaxy of comparable X-ray luminosity, but consistent with the bulk of NLS1 galaxies.

The spectral as well as the variability properties of RGB J0044+193 are indistinguishable from those of radio-quiet NLS1s. In particular, we find no evidence for a flat X-ray component due to inverse Compton emission related to the putative non-thermal radio emission from RGB J0044+193. We argue, however, that this does not rule out a pole-on orientation for RGB J0044+193.

**Key words:** galaxies: abundances – galaxies: individual: RGB J0044+193 – radio lines: general – X-rays: general

## 1. Introduction

The radio-loud X-ray source RGB J0044+193 (R.A. = 00:44:59.12; Dec. = +19:21:40.8; J2000.0) was serendipitously identified as a NLS1 in the course of a large effort to establish a new, well-defined and large sample of X-ray selected BL Lac objects (Laurent-Muehleisen et al. 1998). The basic sample resulted from a cross-correlation of the ROSAT All-Sky Survey and the Green Bank 5GHz radio survey (87GB; Condon et al. 1989). This so-called RGB-sample contains more than 2100 radio-loud X-ray sources and was completely followed-up with the VLA to obtain accurate radio positions and radio core fluxes (Brinkmann et al. 1995, 1997a; Laurent-Muehleisen et al. 1997).

In X-rays NLS1 generally exhibit rapid variability and steep X-ray spectra (e.g. Boller et al. 1996; Brandt et al. 1997; Leighly 1998, 1999). Whether or not the X-ray and optical properties of NLS1 galaxies are affected by orientation is currently the subject of much debate (e.g. Osterbrock & Pogge 1985; Brandt et al. 1997; Boller et al. 1996, 1997). Originally it was suggested that NLS1 are the pole-on versions of regular Seyfert 1 galaxies. This naturally explains the narrower permitted emission lines, if the emission line clouds were confined to a disk perpendicular to the symmetry axis. Orientation dependent emission line properties have also been discussed for other object classes (e.g. Boroson 1992; Baker & Hunstead 1995). The high frequency of soft X-ray excesses seen in NLS1 (e.g. Leighly 1999) also might argue for a face-on orientation, at least in the case of geometrically thick accretion discs (Madau 1988). Further arguments in favor of pole-on geometries are the strong Fe II emission, if it originates in the accretion disc (e.g. Kwan et al. 1995) and the low frequency of warm absorbers in NLS1 (Leighly 1999). Finally, the observed rapid variability as well as absorption features near 1 keV in three NLS1 might be explained by relativistic outflows seen close to the line of sight (Boller et al. 1996; Leighly et al. 1997).

On the other hand, the orientation model would require the hard X-ray spectral index to be orientation dependent, since it is much flatter in broad-line Seyferts than in NLS1. However, current models for the X-ray emission processes predict the opposite behavior (e.g. Haardt & Maraschi 1993). Further, the

extreme variability in IRAS 13224-3809 can be explained by relativistic effects connected with a hot spot at the inner edge of an accretion disc seen under a large inclination angle. Finally, the presence of excess absorption by cold material in the NLS1 Mrk 507 (Iwasawa et al. 1998) and the observation of ionization cones in Mrk 766 (Wilson et al. 1995) argue against a general pole-on orientation for NLS1.

Instead, it has been proposed that NLS1 galaxies are objects with smaller black hole masses and accretion rates closer to the Eddington limit compared to broad-line Seyferts. This scenario naturally explains many of their peculiar optical and X-ray properties (Pounds et al. 1995; Leighly 1999 and references therein).

Radio-loud NLS1 appear to be a rare class of AGN. Apart from RGB J0044+193 there is only one object known, namely PKS 0558-504. The importance of radio-loud NLS1 galaxies lies in the fact that the presence of radio emission and an associated relativistic jet might give us an independent handle on the orientation issue. Hence, the main intention of our ASCA observation was to compare the X-ray properties of the radio-loud NLS1 RGB J0044+193 to radio-quiet NLS1 and to investigate, whether any differences in the X-ray spectrum can be attributed to the radio-loud nature of this object.

## 2. The optical spectrum of RGB J0044+193

The spectrum of RGB J0044+193 shown in Laurent-Muehleisen et al. (1998) and on which its NLS1 classification is based, did not extend far enough to the red to include  $H\alpha$ . We therefore obtained a second spectrum on Sept. 24, 1998 at Lick observatory using the Kast double spectrograph. Two 20 minute exposures were taken to facilitate accurate cosmic ray rejection and the resulting averaged spectrum has a resolution of  $3.8 \text{ \AA}$  and a coverage from 3410 to 8270  $\text{\AA}$  (2900 to 7000  $\text{\AA}$  in the object's rest frame). Weather was variable, but generally poor during the observations. Therefore the flux scale should be taken only as a rough indicator of the source's brightness. Atmospheric lines were removed using an observation of a spectrophotometric standard star. The observations of both source and standard star were done with the slit rotated to the parallactic angle. We did not correct for reddening since the measured  $H\alpha/H\beta$  ratio is consistent with no reddening.

The optical spectrum of RGB J0044+193 appears to be extremely blue (Fig. 1). Even when the contributions from the Balmer continuum, blended Fe emission and possibly Mg II are taken into account, the continuum below 5000  $\text{\AA}$  is still steeper than the limit for a bare accretion disk spectrum ( $\alpha \approx -0.3$ ; e.g. Grupe et al. 1998). This may indicate the presence of additional line emission, perhaps from Fe I (e.g. Kwan et al. 1995), or scattering of a blue intrinsic continuum. If we restrict our measurement of the continuum to the region redward of 5000  $\text{\AA}$ , we find that a power law with a slope<sup>1</sup> of  $\alpha = 1.3$  yields a good fit. For wavelengths blueward of 5000  $\text{\AA}$ , we formally get a slope of  $\alpha = -3.1$ .

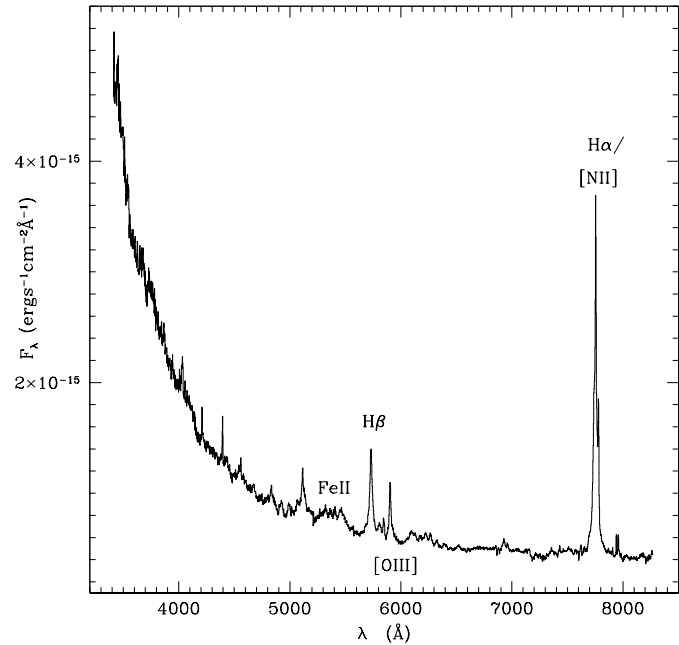


**Fig. 1.** The observed broad band (3410 and 8270  $\text{\AA}$ ) optical spectrum of RGB J0044+193, taken with the Kast double spectrograph at Lick observatory. For clarity, only the emission lines discussed in the text are labeled. Note the extremely blue continuum below 5000  $\text{\AA}$ .

To our knowledge, this is bluest optical continuum of any NLS1 observed to date. It might be speculated that this peculiarity is related to the radio-loudness of RGB J0044+193, for example via optical synchrotron emission from the putative radio jet. However, the spectral shape practically rules out a synchrotron contribution to the blue optical continuum. We further note that the optical continuum of the only other known radio-loud NLS1 PKS 0558-504 is not as blue as that of RGB J0044+193 (Remillard et al. 1986).

The emission line spectrum confirms the original classification as a NLS1 galaxy at redshift of  $z=0.181$ . The broad permitted blend of Fe II emission commonly present in NLS1s severely contaminates the spectrum, making an accurate measurement of the flux and width, in particular of the  $H\beta$  and [O III] lines difficult. In order to account for this, we employ the Fe II subtraction method introduced by Boroson & Green (1992) and now commonly applied (e.g. Leighly 1999). The Fe II emission line spectrum from a high signal-to-noise optical spectrum of the prototype strong Fe emitter I Zw 1 is first convolved with a Gaussian and then scaled until the width and intensity of the lines approximately match those seen in the RGB J0044+193 spectrum. We find that a  $980 \text{ km s}^{-1}$  FWHM Gaussian convolution with a normalization 8% of the absolute flux of I Zw 1 provides the best fit (see Fig. 2). This best-fitting Fe II model was then subtracted and the remaining emission lines examined.

$H\beta$  has a Lorentzian rather than a Gaussian profile, which is typical of the NLS1 class (Goncalves et al. 1998). A Lorentzian profile with a FWHM of  $\sim 1330 \text{ km s}^{-1}$  yields an excellent fit.  $H\alpha$  is blended with [N II], but also shows clear indications of a broad component. Our best fit Lorentzian profile yields a

<sup>1</sup>  $f_\nu \propto \nu^{-\alpha}$

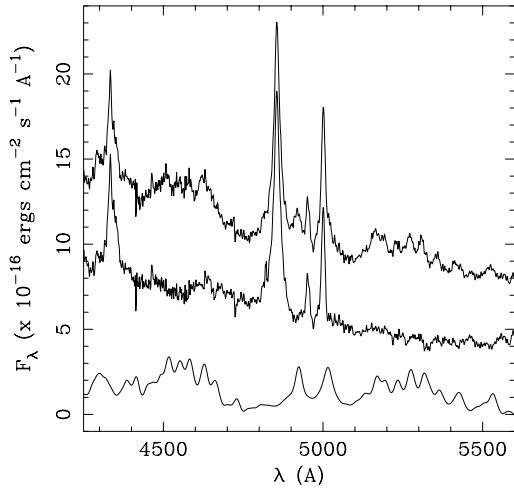


**Fig. 2.** To illustrate the Fe II subtraction procedure, we plot three spectra for RGB J0044+193 between 4300 and 5600 Å in the rest frame of the source. The top one is the observed spectrum. The bottom one is the Fe II model derived from the I Zw 1 template of Boroson & Green (1992) by folding it with a Gaussian of 980 km s<sup>-1</sup> FWHM and normalizing it to about 8% of the flux of I Zw 1. The middle one is the Fe II subtracted spectrum shifted downward by an arbitrary amount for illustrative purposes.

FWHM of 1000 km s<sup>-1</sup>. Considering the degree of blending near H $\alpha$ , this is fully consistent with the dynamics exhibited by the H $\beta$  line. The forbidden [O III] lines are well fit by a Gaussian of FWHM  $\sim$ 750 km s<sup>-1</sup>. This behavior is typical for NLS1s: the broad and narrow components of the permitted lines cannot be clearly separated, but the FWHM is  $<$ 2000 km s<sup>-1</sup>, while the forbidden lines are well-fit by a single narrow component. The final pieces of optical evidence, which support the classification of RGB J0044+193 as a NLS1 are the intensity ratios of the high ionization lines ([O III], [N II]) to the low ionization lines (H $\beta$ , H $\alpha$ ). Because the H $\alpha$ /[N II] emission feature is strongly blended, we cannot determine an accurate flux ratio, but we can confidently say that [N II]/H $\alpha$   $<$  0.4. For [O III]/H $\beta$  we derive a value of 0.2. Both these measurements are consistent with the low values typical for other NLS1 galaxies (Osterbrock & Pogge 1985; Goodrich 1989), and significantly lower than those exhibited by quasars, where [O III]/H $\beta$   $>$  3.0 and [N II]/H $\alpha$   $>$  0.75.

### 3. The radio source associated with RGB J0044+193

Applying the criterium of Kellerman et al. (1989), who define  $R = 10$  as the dividing line between radio-loud and radio-quiet quasars<sup>2</sup>, the source is radio-loud, since the ratio of the total 4.85 GHz radio flux from the 87GB survey ( $f_{4.85\text{GHz}} = 24$  mJy) and the optical magnitude ( $m_O = 16.7$ ) is  $R \approx 31$ . The radio flux corresponds to a luminosity<sup>3</sup> of  $\log P = 24.5$  W Hz<sup>-1</sup>. Thus, also using luminosity criteria (e.g. Joly 1991; Miller et al. 1993), RGB J0044+193 should be classified as a radio-loud AGN.

<sup>2</sup>  $R$  is defined as the  $K$ -corrected ratio of the 4.85 GHz radio flux and the optical flux at 4400 Å.

<sup>3</sup>  $H_0 = 50$  km s<sup>-1</sup> Mpc<sup>-1</sup>,  $q_0 = 0.5$ .

In general, NLS1 galaxies are considered to be radio-quiet AGN. Ulvestad et al. (1995) investigated the radio emission of 15 NLS1 galaxies with the VLA down to a flux limit of 0.25 mJy at 5 GHz. They found luminosities (or upper limits) between  $\log P = 20.5$  W Hz<sup>-1</sup> and  $\log P = 22.5$  W Hz<sup>-1</sup>. Thus, RGB J0044+193 is about two orders of magnitude brighter at 4.85 GHz than any of the objects in the sample of Ulvestad et al. (1995). Comparing the radio-loudness  $R$  of RGB J0044+193 to that of the Ulvestad et al. (1995) sources, we again find that it is a factor of  $\sim 6$  higher than any of those. Even if we use the lower flux from the VLA measurement (see below)  $R$  is higher by a factor of two. However, in this case  $R < 10$  and hence RGB J0044+193 is technically radio-quiet (but confer discussion below). There is only one other radio-loud NLS1 galaxy known up to now (PKS 0558-504) and we compare it to RGB J0044+193 in Sect. 7.1.

The radio luminosity of RGB J0044+193 is much larger than usually detected in normal galaxies or starbursts. Smith et al. (1998), for example, study the 20 most radio luminous starburst galaxies from the UGC sample. The average 4.85 GHz luminosity of this sample is  $\langle \log P \rangle \approx 23$ , and even the radio brightest object is more than a factor of five less luminous than RGB 0044+193. Therefore, any significant contribution to the total radio emission other than non-thermal radiation from a radio jet seems rather unlikely.

Interestingly, RGB J0044+193 was detected with a 4.85 GHz flux of only 7 mJy in the high resolution follow-up observation with the VLA (Laurent-Muehleisen et al. 1997). This indicates that the source is either extended or variable. The latter is supported by two additional pieces of evidence: firstly, the radio source appears unresolved on the VLA map and secondly, it is not detected in the NRAO/VLA Sky Survey (NVSS; Condon et al. 1998) at 1.4 GHz, which is sensitive down to  $\sim 2.5$  mJy. Given that extended radio emission generally shows steep radio spectra, the 1.4 GHz radio flux should have been higher than 7 mJy and hence easily detectable in the NVSS. Unfortunately, existing radio data do not allow us to place limits on the likelihood for large intrinsic radio variability in NLS1 galaxies as a class. Even in the case of RGB J0044+193 the true amount of intrinsic variability is uncertain, since the sense of the differences between the 87GB and the VLA measurements is the same as if overresolution were a problem. Due to the compactness of the radio source interstellar scintillation might also be relevant.

If taken at face value, the data also imply an inverted spectrum between 4.85 and 1.4 GHz, probably due to synchrotron self-absorption. This would be consistent with the observed unresolved compact radio core. Note that neither PKS 0558-504 nor the Ulvestad et al. (1995) sources show inverted spectra.

### 4. The ASCA observation

RGB J0044+193 was observed with ASCA (Tanaka et al. 1994) in 1-CCD faint mode from January 9, 08:55:23 to January 10, 23:49:13 (UT) 1998.

The data were analysed using FTOOLS 4.1. The recommended standard screening criteria were applied to the data. For the GIS the minimum elevation angle above the Earth's limb (ELV) was chosen to be  $5^\circ$ . In the case of the SIS we used  $\text{ELV} > 10^\circ$ . To avoid atmospheric contamination, data were only accepted in the SIS when the angle between the target and the bright earth (BR\_EARTH) was greater than  $20^\circ$ . Further, a minimum cut-off rigidity (COR) of 6 GeV/c was applied for both, the SIS and the GIS. Data taken within 60 seconds after passage of the day-night-terminator and the South Atlantic Anomaly (SAA) were not considered in the analysis. Periods of high background were manually excluded from the data by checking the light curve of the observation. The resulting effective exposures were 47.9 ksec for each GIS and 45.1 and 46.4 ksec for SIS0 and SIS1, respectively.

Source counts were extracted from a circular region centered on the target with a radius of  $6'$  for the GIS and  $4'$  for the SIS. We used the local background determined from the observation in the analysis for both detectors. In particular, the GIS background was estimated from a source free region at the same off-axis angle as the source and with the same size as the source extraction region. In total,  $\sim 2500$  counts were detected from RGB J0044+193 in each of the SIS detectors. Because of the steep spectrum and the lower effective area, the number of photons detected with the GIS detectors was a about factor of two smaller.

All spectra were rebinned to have at least 20 photons in each energy channel. This allows the use of the  $\chi^2$  technique to obtain the best fit values for the model spectra. We used the latest GIS redistribution matrices available (V4.0) from the calibration database and created the SIS response matrices for our observation using SISRMG, which applies the latest charge transfer inefficiency (CTI) table (`sisph2pi_110397.fits`). The ancillary response files for all four detectors were generated using the ASCAARF program.

Spectra were fitted in the energy range 0.8 to 8 keV for both GIS. For SIS0 and SIS1 we used 0.5 to 7 keV and 0.7 to 7 keV, respectively. The upper energy boundaries are given by the maximum energy at which the source was detected in each instrument. The lower energy boundaries result from the calibration uncertainties of the detectors. In particular, SIS1 recently shows systematic residuals below 0.6 keV (Dotani et al. 1997). Also, since the CCD temperature of SIS1 was higher than SIS0 during the observation, we decided to ignore the data below 0.7 keV for SIS1. An increasing RDD (Residual Dark Distribution), which is caused by radiation damage, has been reported for both CCDs. This effect cannot be corrected for with currently available software. RDD degradation should be negligible for 1-CCD observations, however (Dotani et al. 1997).

## 5. Spectral analysis

Since the spectral fitting for the individual detectors gives consistent results, we only cite the parameters for all four detectors fitted simultaneously in the following. The normalization of the GIS detectors was allowed to vary with respect to the SIS, be-

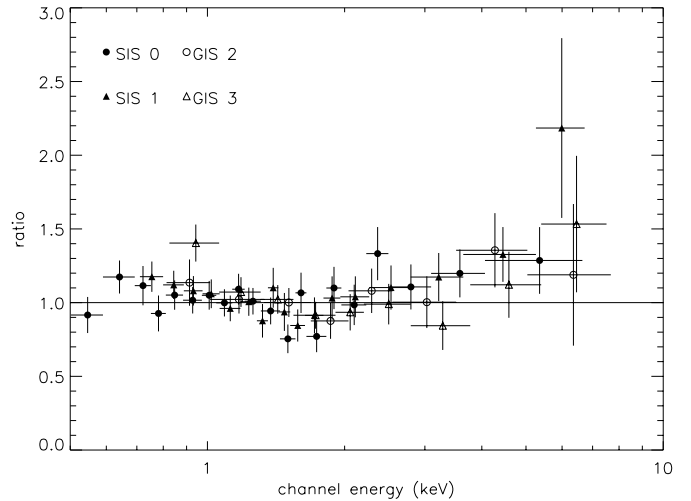


**Fig. 3.** Ratio of the data to a simple power law model. The break in the X-ray spectrum around 1.8 keV can clearly be seen.

cause of the known cross-calibration uncertainties. The resulting differences in the normalization between the SIS and the GIS detectors are of the order of 5 to 10%.

We first investigated a simple power law model with the absorption fixed to the Galactic value ( $N_H = 3.55 \times 10^{20} \text{ cm}^{-2}$ ). The resulting best fit parameters are  $\Gamma = 2.47 \pm 0.07$  and  $\chi^2 = 405.5$  (360 d.o.f.). The ratio of the data to this model is shown in Fig. 3. It can clearly be seen that there is a significant break in the spectrum of RGB J0044+193 around 1.8 keV.

Next we fitted the spectrum with a broken power law model. To put tighter constraints on the break energy and the low energy power law, we first fitted a simple power law model to the data above 2 keV and fixed the resulting high energy power law ( $\Gamma \approx 2.1$ ) in the broken power law fit. This gives  $\Gamma_{\text{low}} = 2.69 \pm 0.11$ ,  $E_{\text{break}} = 1.79_{-0.20}^{+0.35} \text{ keV}$  and  $\chi^2 = 386.5$  (359 d.o.f.). The difference in  $\chi^2$  is significant at more than 99.9% confidence according to a F-test.

An even better fit results when a blackbody model superimposed on a simple power law is applied instead of a broken power law. Using ZBBODY we get (again for fixed Galactic absorption)  $T = 0.19 \pm 0.02 \text{ keV}$  for a power law photon index of  $\Gamma = 2.1$  (fixed). The resulting  $\chi^2$  is 382.6 for 359 degrees of freedom. The resulting ratio of data to model is shown in Fig. 4. For this model we get a 2–10 keV flux of  $(7.9 \pm 0.3) \times 10^{-13} \text{ erg cm}^{-2} \text{ s}^{-1}$ , which gives a rest frame 2–10 keV luminosity of  $(1.35 \pm 0.05) \times 10^{44} \text{ erg s}^{-1}$ . The corresponding soft X-ray (0.5–2 keV) luminosity is  $1.9 \times 10^{44} \text{ erg s}^{-1}$ .

Alternatively, if we use a thermal bremsstrahlung model (ZBREMSS) instead of a blackbody, we also get an acceptable fit and the best fitting parameters are  $T = 0.45_{-0.07}^{+0.10} \text{ keV}$ ,  $\Gamma = 2.1$  (fixed) and  $\chi^2 = 385.9$  (359 d.o.f.). We note that leaving the photon index as a free parameter in these models gives values that are consistent with the photon index determined at higher energies.

We do not detect any indication of absorption edges due to O VII and O VIII and the upper limits on the optical depths are

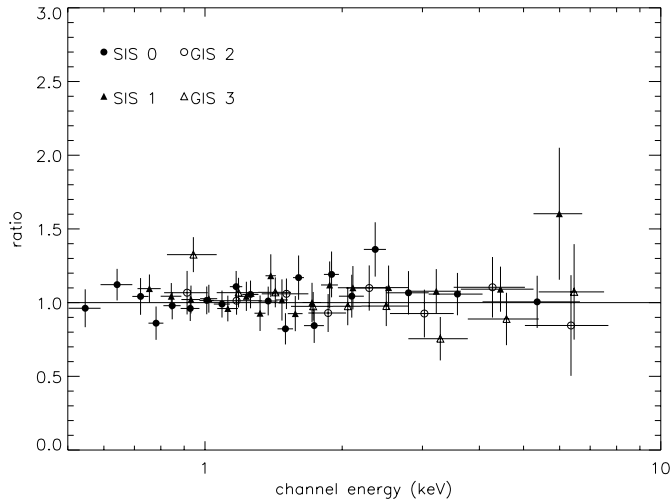


**Fig. 4.** Ratio of the data to a model including a blackbody with  $T = 0.19 \pm 0.02$  keV and a power law with a photon index of  $\Gamma = 2.1$ .

$\tau(\text{OVII}) < 0.50$  and  $\tau(\text{OVIII}) < 0.54$ . We also searched for a  $K\alpha$  emission line from neutral or ionized iron, but could not find any. Due to the low photon statistics at high energies the upper limits on the equivalent widths are not very stringent: 250 eV and 400 eV for a narrow emission line at 6.4 and 6.7 keV, respectively.

## 6. The light curve

The background subtracted light curve of RGB J0044+193 in the 0.5–7.0 keV energy range during the ASCA observation is shown in Fig. 5. The data were binned in such a way that each data point corresponds to one orbit of the satellite. For clarity, only the combined SIS0/SIS1 light curve is shown, but we note that the same qualitative behavior is also seen in the GIS detectors.

The source count rate was clearly higher at the beginning of the observation. It decreased by a factor of two within one day. There is also evidence for significant variability on much shorter time scales, albeit with smaller amplitudes.

In the ROSAT All-Sky Survey RGB J0044+193 was detected with a PSPC count rate of  $0.17 \pm 0.02$  counts  $\text{s}^{-1}$ . Using a power law model with  $\Gamma = 2.7$ , this results in an unabsorbed 0.1–2.4 keV flux of  $(4.8 \pm 0.6) \times 10^{-12}$  erg  $\text{cm}^{-2}$   $\text{s}^{-1}$ . This value is consistent with the corresponding ASCA flux for the broken power law model in the same energy range  $((5.2 \pm 0.2) \times 10^{-12}$  erg  $\text{cm}^{-2}$   $\text{s}^{-1}$ ).

A common measure of AGN X-ray variability is the excess variance  $\sigma_e$  (Nandra et al. 1997; Leighly 1999). Basically it measures the variance of the light curve minus the variance due to the measurement errors. For exposures of similar duration it is also a measure of the variability time scale. In the case of RGB J0044+193 we calculate  $\sigma_e = 0.045 \pm 0.014$ , which is significantly higher than the values found for broad-line Seyfert 1 galaxies of similar X-ray luminosity, but consistent with the values found for other NLS1s (Leighly 1999). This is illustrated in Fig. 6 (adapted from from Fig. 3 of Leighly 1999), which

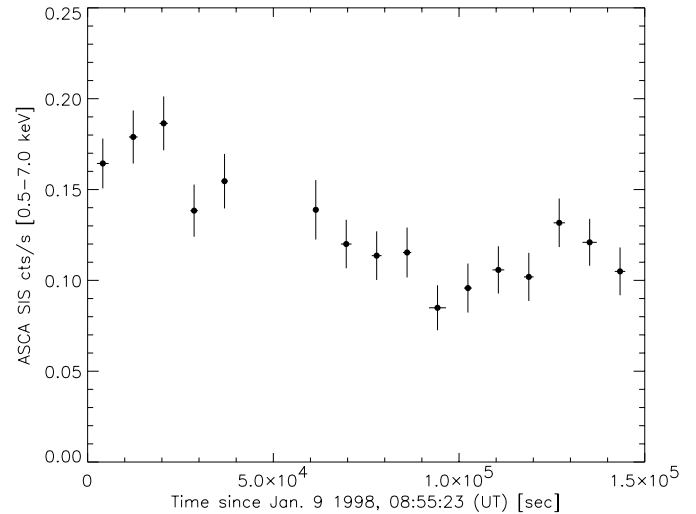


**Fig. 5.** X-ray light curve of RGB J0044+193 for the combined SIS detectors in the 0.5 to 7 keV range.

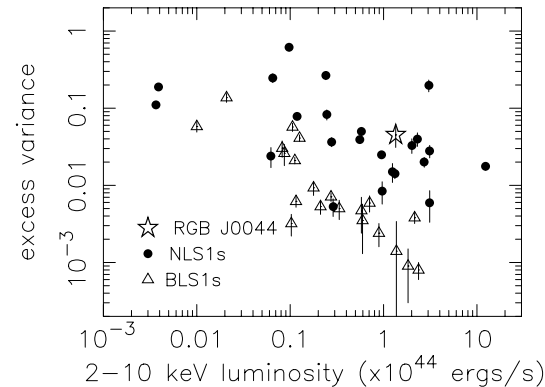


**Fig. 6.** Excess variance vs. 2–10 keV luminosity for RGB J0044+193 compared with broad-line and narrow-line Seyfert 1 galaxies; figure taken from Leighly (1999). At a given X-ray luminosity NLS1 galaxies clearly show more rapid variability than broad line objects (see also Leighly 1998). RGB J0044+193 falls into the region of NLS1 galaxies, thus providing independent evidence for the NLS1 nature of RGB J0044+193.

shows the excess variance of RGB J0044+193 in the total band in comparison to broad-line and narrow-line Seyfert 1 galaxies.

Given the evidence for a soft component in the X-ray spectrum of RGB J0044+193, we also calculated the excess variance above and below 1.8 keV. We get  $0.040 \pm 0.014$  at low energies and  $0.093 \pm 0.031$  at higher energies. Although there seems to be a tendency for more pronounced variability at higher energies, we do not consider the difference in the excess variances of the soft and the hard band as significant.

## 7. Comparison to other NLS1 galaxies

### 7.1. The second radio-loud NLS1 PKS 0558-504

The only other known radio-loud NLS1 galaxy is PKS 0558-504. It is at a redshift of  $z = 0.137$ , has a optical magnitude of  $m_B = 14.97$  and a 4.85 GHz radio flux of 113 mJy. This

gives a radio-loudness of  $R \approx 27$  and a radio luminosity of  $\log P = 24.9$ . These parameters are very similar to those of RGB J0044+193.

In X-rays, PKS 0558-504 is an order of magnitude more luminous than RGB J0044+193. Leighly (1999) gives a 0.5–2 keV luminosity of  $\approx 1.7 \times 10^{45} \text{ erg s}^{-1}$  (as compared to  $1.9 \times 10^{44} \text{ erg s}^{-1}$  for RGB J0044+193). Despite this huge difference in luminosity, the ASCA spectra of the two radio-loud NLS1 galaxies are remarkably similar. Leighly (1999) finds a slightly higher temperature ( $kT \approx 0.25 \text{ keV}$ ) for the blackbody model and a slightly steeper hard photon index ( $\Gamma \approx 2.25$ ). Interestingly, the spectrum of PKS 0558-504 also shows marginal evidence for an emission line around 6.7 keV with an equivalent width of about 100 eV, which is well below the upper limit for RGB J0044+193, however.

### 7.2. Radio-quiet NLS1s

It was shown by Brandt et al. (1997), that the hard (2–10 keV) X-ray spectrum of NLS1 galaxies is steeper on average than that of broad line Seyfert 1 galaxies, although the scatter in spectral indices seems to be smaller compared to ROSAT PSPC measurements (Boller et al. 1996). Our result for the photon index of RGB J0044+193 at energies above 2 keV ( $\Gamma \approx 2.1$ ) is close to the average value for NLS1 (Brandt et al. 1997; Leighly 1999). Although the hard X-ray spectra of NLS1 galaxies are significantly steeper than those of normal Seyfert 1 galaxies, they are nevertheless much flatter than the soft X-ray spectra of NLS1 galaxies as measured with ROSAT. This clearly indicates a break in the X-ray spectrum. In Sect. 5 we have presented unambiguous evidence for the presence of such a break in RGB J0044+193 and the ASCA photon index below the break energy ( $\Gamma_{\text{low}} \approx 2.7$ ) is consistent with the ROSAT spectral indices of NLS1 galaxies (Boller et al. 1996). Similar energy breaks are found in a systematic study of the ASCA spectra of NLS1 galaxies (Leighly 1999). We conclude that the X-ray spectral properties of RGB J0044+193 do not appear to be different from radio-quiet NLS1 galaxies.

For radio-loud AGN a correlation between the core-dominance and the X-ray spectral index has been claimed in the sense that the most core-dominated sources have the flattest X-ray spectra (e.g. Kembhavi 1993; Brinkmann et al. 1997b). This result is usually interpreted in terms of a flat inverse Compton component in the X-ray spectrum, which is related to the relativistic radio jet and which dominates the emission spectrum for objects oriented close to the line of sight. The seed photons for this process are either the synchrotron photons generated in the radio jet itself or external photons from the accretion disc or the emission line regions. In this scenario, the apparent absence of a flat X-ray component in RGB J0044+193 might indicate that the radio jet is oriented at a rather large angle to the line of sight, which would argue against a pole-on geometry at least for this source. However, there are several caveats. First of all, nothing is known about the physical parameters related to the putative radio jet in RGB J0044+193 or NLS1s in general. They might be different from those in radio-loud quasars.

Secondly, RGB J0044+193 is barely radio-loud. Therefore any inverse Compton component (e.g. synchrotron self-Compton) might simply be too weak to be detected in our ASCA observation.

Fig. 6 illustrates that RGB J0044+193 is significantly more variable than Seyfert 1 galaxies of the same X-ray luminosity. The excess variance is more than one order of magnitude larger. In fact, RGB J0044+193 clearly falls into the region populated by the bulk of NLS1 galaxies (Leighly 1999). Also in terms of their variability properties, there seems to be no difference between RGB J0044+193 and radio-quiet NLS1 galaxies.

## 8. Summary

We presented radio, optical and X-ray data of the peculiar radio-loud NLS1 galaxy RGB J0044+193. The results can be summarized as follows:

1. The radio observations indicate significant variability in the flux from the compact radio source associated with RGB J0044+193 and evidence for an inverted radio spectrum.
2. The optical spectrum clearly confirms the NLS1 classification for RGB J0044+193. In addition, the optical continuum appears to be extremely blue. This might indicate additional line emission or scattering of a blue intrinsic continuum.
3. The X-ray spectrum obtained with the ASCA satellite shows a break near 2 keV. At higher energies it is best described by a power law model with a photon index of  $\Gamma = 2.1$ . The soft component can be modeled with either a  $\sim 0.2 \text{ keV}$  blackbody or a steeper power law ( $\Gamma \approx 2.7$ ).
4. The ASCA SIS count rate decreases by a factor of two within one day and there is evidence for variability with lower amplitude on much smaller time scales. The variability behavior is characterized by an excess variance of  $0.045 \pm 0.014$ .

Both the spectrum and the variability properties are typical for NLS1 galaxies, which provides independent evidence for the classification of RGB J0044+193. We do not detect any differences between RGB J0044+193 and the bulk of radio-quiet NLS1 galaxies. In particular, we find no evidence for a flat X-ray component due to inverse Compton emission related to the putative non-thermal radio emission of RGB J0044+193. This does not necessarily argue against a pole-on orientation for RGB J0044+193, however. It might well be possible that the physical parameters of the putative radio jet in this source render an inverse Compton component undetectable within our ASCA observation.

*Acknowledgements.* JS acknowledges financial support from the RIKEN–MPG exchange program. JS also thanks his colleagues from the Cosmic Radiation Laboratory at RIKEN for hospitality and support during a stay at the institute, where part of this work was done. We wish to thank Michael Brotherton for useful discussions on iron template line fitting. KML gratefully acknowledges support through NAG5-7261 (ASCA). SALM acknowledges support from the Department of Energy at the Lawrence Livermore National Laboratory under contract W-7405-ENG-48. This research has made use of the ASCA

IDL Analysis System developed by Tahir Yaqoob, Peter Serlemitsos and Andy Ptak and of the NASA/IPAC Extragalactic Data Base (NED), which is operated by the Jet Propulsion Laboratory, California Institute of Technology, under contract with the National Aeronautics and Space Administration.

## References

- Baker J.C., Hunstead R.W., 1995, *ApJ* 452, L95  
 Boller Th., Brandt W.N., Fink H.H., 1996, *A&A* 305, 53  
 Boller Th., Brandt W.N., Fabian A.C., Fink H.H., 1997, *MNRAS* 289, 393  
 Boroson T.A., 1992, *ApJ* 399, L15  
 Boroson T.A., Green R.F., 1992, *ApJS* 80, 109  
 Brandt W.N., Mathur S., Elvis M., 1997, *MNRAS* 285, 25P  
 Brinkmann W., Siebert J., Reich W., et al., 1995, *A&AS* 109, 147  
 Brinkmann W., Siebert J., Feigelson E.D., et al., 1997a, *A&A* 323, 739  
 Brinkmann W., Yuan W., Siebert J., 1997b, *A&A* 319, 413  
 Condon J.J., Broderick J.J., Seielstad G.A., 1989, *AJ* 97, 1064  
 Condon J.J., Cotton W.D., Greisen E.W., et al., 1998, *AJ* 115, 1693  
 Dotani T., Yamashita A., Ezuka H., et al., 1997, *ASCA News* No. 5  
 Goncalves A.C., Véron P., Véron-Cetty M.-P., 1998, In: Gaskell C.M., Brandt W.N., Dietrich M., Dultzin-Hacyan D., Eracleus M. (eds.) *Structure and Kinematics of the Quasar Broad Line Regions*. In press  
 Goodrich R.W., 1989, *ApJ* 342, 224  
 Grupe D., Beuermann K., Thomas H.-C., Mannheim K., Fink H.H., 1998, *A&A* 330, 25  
 Haardt F., Maraschi L., 1993, *ApJ* 413, 507  
 Iwasawa K., Brandt W.N., Fabian A.C., 1998, *MNRAS* 293, 251  
 Joly M., 1991, *A&A* 242, 49  
 Kellermann K.I., Sramek R., Schmidt M., Shaffer D.B., Green R., 1989, *AJ* 98, 1195  
 Kembhavi A., 1993, *MNRAS* 264, 683  
 Kwan J., Cheng F., Fang L., Zheng W., Ge J., 1995, *ApJ* 440, 628  
 Laurent-Muehleisen S.A., Kollgaard R.I., Ryan P.J., et al., 1997, *A&AS* 122, 235  
 Laurent-Muehleisen S.A., Kollgaard R.I., Ciardullo R.B., et al., 1998, *ApJS* 118, 127  
 Leighly K.M., 1998, In: Holt S.S., Kallman T.R. (eds.) *Proc. Accretion Processes in Astrophysical Systems: Some Like it Hot!* Woodbury, New York, p. 199  
 Leighly K.M., 1999, *ApJ* submitted  
 Leighly K.M., Mushotzky R.F., Nandra K., Forster K., 1997, *ApJ* 489, L25  
 Madau P., 1988, *ApJ* 327, 116  
 Miller P., Rawlings S., Saunders R., 1993, *MNRAS* 263, 425  
 Nandra K., George I.M., Mushotzky R.F., Turner T.J., Yaqoob T., 1997, *ApJ* 476, 70  
 Osterbrock D.E., Pogge R.W., 1985, *ApJ* 297, 166  
 Pounds K.A., Done C., Osborne J.P., 1995, *MNRAS* 277, 5P  
 Remillard R.A., Bradt H.V., Buckley D.A.H., et al., 1986, *ApJ* 301, 742  
 Smith D.A., Herter T., Haynes M.P., 1998, *ApJ* 494, 150  
 Tanaka Y., Inoue H., Holt S.S., 1994, *PASJ* 46, L37  
 Ulvestad J.S., Antonucci R.R.J., Goodrich R.W., 1995, *AJ* 109, 81  
 Wilson, A.S., 1995, In: Ward M.J. (ed.) *Proceedings of the Oxford Torus Workshop*. p. 55